

Site dependence of large oxygen isotope effect in $Y_{0.7}Pr_{0.3}Ba_2Cu_3O_{6.97}$

Guo-meng Zhao*

Morris Research, Inc., 44 Marguerita Road, Kensington, California 94707

Joel W. Ager III

Center for Advanced Materials, Lawrence Berkeley Laboratory, Berkeley, California 94720

Donald E. Morris

Morris Research, Inc., 44 Marguerita Road, Kensington, California 94707

(Received 11 April 1996)

We report site-selective oxygen isotope effects on T_c and penetration depth in $Y_{0.7}Pr_{0.3}Ba_2Cu_3O_{6.97}$ and in $YBa_2Cu_3O_{7-\delta}$. In Pr-substituted (underdoped) samples with ^{18}O in only the CuO_2 plane-sites, the T_c shift was -1.46 K vs -1.7 K for ^{18}O at all sites; the α_O values are 0.2 and 0.24. The corresponding T_c shifts in pure $YBa_2Cu_3O_{7-\delta}$ were -0.24 K and -0.3 K. The shift is dominated by CuO_2 planar oxygen mass in both compounds, and not by the apical sites. Thus, apical site isotope induced charge transfer to CuO_2 planes does not seem a viable explanation for the isotope effects in YBCO. Our results indicate that the oxygen related phonons in the CuO_2 planes play a significant role in the pairing mechanism. [S0163-1829(96)01129-0]

The pairing mechanism responsible for high- T_c superconductivity in cuprates is still an open question. In conventional superconductors, the dependence of the transition temperature $T_c \propto M^{-\alpha}$ on the ion mass M gives strong evidence for phonon-mediated pairing if $\alpha \approx 0.5$. A small oxygen isotope effect on T_c was observed in optimally doped cuprates, while a large oxygen isotope effect was found in underdoped cuprates.¹⁻⁸ The large oxygen isotope effect in the underdoped regime may suggest an important role of the phonons in the pairing mechanism.

However, attempts have been made to argue against the importance of the phonons by explaining these isotope results as due to a dependence of the hole concentration on the mass of the apical oxygen.⁹ If this explanation were correct, one would expect a large oxygen isotope effect on the penetration depth for the fully ^{18}O -substituted samples, but a negligible isotope effect on the penetration depth for the site-selectively substituted samples where ^{18}O atoms are in the plane sites and ^{16}O atoms in the apical and chain sites. There would also be a negligible oxygen isotope shift for the underdoped plane-site ^{18}O -substituted samples if the above explanation were correct. So measurements of site-selective oxygen isotope effects on T_c and the penetration depth in underdoped and optimally doped cuprates will distinguish which oxygen is responsible for these isotope effects and eventually pinpoint the pairing mechanism of high- T_c superconductivity.

The site-selective oxygen isotope effect on T_c has been recently measured for overdoped³ and optimally doped¹⁰ $YBa_2Cu_3O_y$. For overdoped $YBa_2Cu_3O_7$, Nickel *et al.*³ have observed a small negative oxygen isotope effect on T_c when the ^{18}O samples contain $\sim 95\%$ ^{18}O in the CuO_2 plane sites and primarily ^{16}O in the apical and chain sites. For optimally doped $YBa_2Cu_3O_{6.96}$, Zech *et al.*¹⁰ have, however, found a positive isotope effect on T_c when only planar ^{16}O is exchanged by ^{18}O . The reason for the above discrepancy may be that the superconducting transition of the site-selective

isotope samples in Ref. 3 is too broad to be reliably defined. Since the site-selective isotope shifts in optimally doped and overdoped $YBa_2Cu_3O_y$ are so small and could be explained by any conventional or unconventional model, these results cannot effectively show whether the phonons are important in the pairing mechanism, and which phonons play a dominant role if they are significant in the pairing. For underdoped cuprates, the oxygen isotope shift is, however, large, making them attractive candidates to study the contributions of the oxygen isotope effects from the different oxygen sites. Here we report site-selective oxygen isotope effects on T_c and the penetration depth in $Y_{1-x}Pr_xBa_2Cu_3O_{6.97}$ with $x=0.0$ and 0.3 . The results clearly show that the oxygen in the CuO_2 plane sites predominantly contributes to the total oxygen isotope effects on the penetration depth and T_c in both optimally doped $YBa_2Cu_3O_y$ and underdoped $Y_{0.7}Pr_{0.3}Ba_2Cu_3O_y$.

The samples were prepared from high-purity Y_2O_3 (99.99%), Pr_6O_{11} (99.999%), $BaCO_3$ (99.9999%), and CuO (99.9999%). The well-ground powder mixtures were calcined at $920^\circ C$ for 15 h in flowing oxygen ($70\text{ cm}^3/\text{min}$). The samples were ground, pelletized, and then sintered at $920^\circ C$ for 15 h in flowing oxygen. To ensure that the samples have small grain size and enough porosity, they were reground thoroughly, pelletized, annealed in flowing oxygen at $800^\circ C$ for 10 h, and cooled to room temperature in a rate of $50^\circ C/h$. The resulting pellets have mass density of $\sim 4.0\text{ g/cm}^3$, which is $\sim 60\%$ of the theoretical density.

The pelletized samples were broken into halves, and the halves were subject to ^{16}O and ^{18}O isotope diffusion, which was conducted in two parallel quartz tubes separated by about 2 cm .^{3,5} The diffusion was carried out for 20 h at $670^\circ C$ and oxygen pressure of ~ 1.0 bar. The cooling time from 670 to $120^\circ C$ was 11 h ($50^\circ C/h$). The oxygen isotope enrichment was determined from the weight changes of both ^{16}O and ^{18}O samples (the weights decreased by $\sim 0.15\%$ for the ^{16}O samples and increased by $\sim 1.9\%$ for the ^{18}O

samples). The ^{18}O samples had $\sim 95\%$ ^{18}O and $\sim 5\%$ ^{16}O . The lattice constants for the $x=0$ samples were determined to be $a=3.821 \text{ \AA}$, $b=3.884 \text{ \AA}$, and $c=11.687 \text{ \AA}$, corresponding to an oxygen content of 6.94 ± 0.02 .¹¹ For the Pr-doped samples, the oxygen content may be slightly larger than the pure samples, but the same oxygen content (~ 6.94) as the pure samples will be used for the later calculation.

The site-selectively isotope-substituted samples were obtained by annealing both the ^{16}O and ^{18}O standard samples together at $320 \text{ }^\circ\text{C}$ for 100 h in flowing oxygen. After this treatment, the weights of the ^{16}O samples decreased by $\sim 0.05\%$, while the weights of the ^{18}O samples decreased by 0.78% for $x=0$ and by 0.84% for $x=0.3$. Normally, right after being taken out of the furnace, the weight loss of the ^{16}O samples is $\sim 0.10\text{--}0.15\%$ (due to loss of water and CO_2 , etc.) if the oxygen content remains the same after annealing. For the site-selective ^{16}O samples, the weight loss is only $\sim 0.05\%$, which is $\sim 0.05\text{--}0.10\%$ less than the normal weight loss. This implies that the oxygen content increases by $\sim 0.02\text{--}0.04$ after annealing at $320 \text{ }^\circ\text{C}$ for 100 h. Then we calculate that $\sim 2.66/6.97$ and $\sim 2.92/6.97$ of the ^{18}O atoms are exchanged back to the ^{16}O atoms for $x=0.0$ and 0.3 , respectively. Since the isotope exchange primarily occurs to the chain and apical oxygen sites below $330 \text{ }^\circ\text{C}$,¹² the above weight-change results imply that the site-selectively substituted ^{18}O samples contain primarily ^{16}O in the apical and chain sites, and $\sim 95\%/85\%$ ^{18}O in the planar sites for $x=0.0/0.3$.

Site occupancy of the ^{16}O and ^{18}O oxygen isotopes was also checked by Raman spectroscopy. Raman spectra were generated by the 488-nm line of an Ar^+ laser, focused to a 15-mm spot. Typical collection times were $5\text{--}7$ min at an instrumental resolution of 2.5 cm^{-1} . Figures 1(a) and 1(b) show the Raman spectra of the site-selective ^{16}O and ^{18}O samples with $x=0.0$ and 0.3 . For the site-selective $\langle ^{18}\text{O}_p \text{ } ^{16}\text{O}_{ac} \rangle$ samples (where p means plane, ac means apical/chain), the 500-cm^{-1} peak (corresponding to the motion of the apical oxygen) has no observable shift while the 337- or 317-cm^{-1} peak (corresponding to the motion of the planar oxygen) is shifted by $22 \pm 2 \text{ cm}^{-1}$ for $x=0$ and by $17 \pm 3 \text{ cm}^{-1}$ for $x=0.3$. The Raman results thus confirm that the $\langle ^{18}\text{O}_p \text{ } ^{16}\text{O}_{ac} \rangle$ samples contain primarily ^{16}O in the apical and chain sites and $\sim (100 \pm 10\%)/(85 \pm 15\%)$ ^{18}O in the planar sites for $x=0.0/0.3$. The consistent determinations of the oxygen isotope enrichments from the weight changes and Raman spectra imply that the site-selectively oxygen isotope exchange is done uniformly throughout the samples, in agreement with Ref. 12.

The susceptibility was measured with a quantum design superconducting quantum interference device (SQUID) magnetometer. The field-cooled, measured-on-warming (FCW) susceptibility was measured in a field of $\sim 10 \text{ Oe}$. For the $x=0$ samples, the temperature measurements were performed with a platinum resistance thermometer (Lakeshore PT-111) placed in direct contact with the sample and driven by microprocessor controlled ac bridge in the SQUID magnetometer. The resolution is 2.5 mK and the reproducibility is 10 mK at 77 K after cycling to room temperature. The magnetic field was kept unchanged throughout the whole series of measurements.

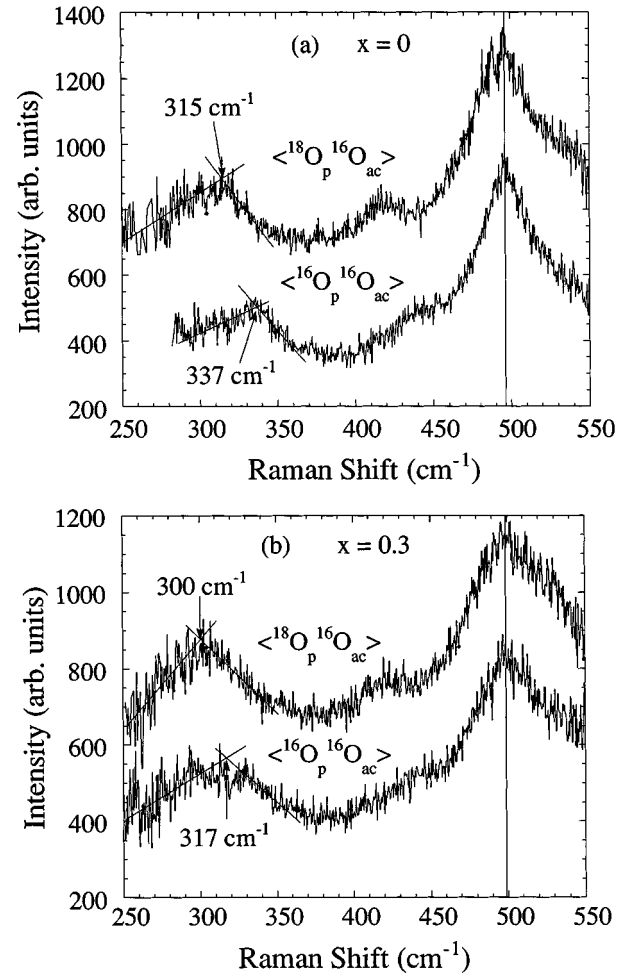


FIG. 1. The Raman spectra of the site-selective ^{16}O and ^{18}O samples with (a) $x=0.0$ and (b) $x=0.3$. For the site-selective $\langle ^{18}\text{O}_p \text{ } ^{16}\text{O}_{ac} \rangle$ samples, the 500-cm^{-1} peak (corresponding to the motion of the apical oxygen) has no observable shift, while the 337- or 317-cm^{-1} peak (corresponding to the motion of the planar oxygen) is shifted by $22 \pm 2 \text{ cm}^{-1}$ for $x=0.0$ and by $17 \pm 3 \text{ cm}^{-1}$ for $x=0.3$. The Raman shifts are consistent with the weight-change measurements, implying that the oxygen loading is done uniformly throughout the samples at low temperatures (e.g., $320 \text{ }^\circ\text{C}$). The peak positions defined in this way are only for the deduction of the relative Raman shifts.

In Figs. 2(a) and 2(b), we show the susceptibility near T_c for (a) the standard ^{16}O and ^{18}O samples of $\text{YBa}_2\text{Cu}_3\text{O}_{6.94}$ and (b) the site-selective ^{16}O and ^{18}O samples of $\text{YBa}_2\text{Cu}_3\text{O}_{6.97}$. The T_c shift of the plane-site ^{18}O -substituted sample is -0.25 K , while the T_c shift of the fully ^{18}O -substituted sample is -0.30 K . The result indicates that the main contribution ($>80\%$) to the oxygen isotope shift comes from the planar oxygen, in agreement with Ref. 10.

From Figs. 2(a) and 2(b), we also note that there are well-defined linear portions on the transition curves just $\sim 0.5 \text{ K}$ below the diamagnetic onset temperatures. The negative curvature near T_c ($\sim 0.5\text{-K}$ range) is due to $H_{\text{ext}} > H_{c1}(T)$ and to the fluctuation and/or inhomogeneity. It is evident that the slope (denoted by P_1) of the linear portion for the standard ^{18}O sample is $\sim 6.8 \pm 1.0\%$ smaller than for the standard ^{16}O sample, while the slope for the site-selective ^{18}O sample is $\sim 4.0 \pm 1.0\%$ smaller than for the ^{16}O sample. The procedures

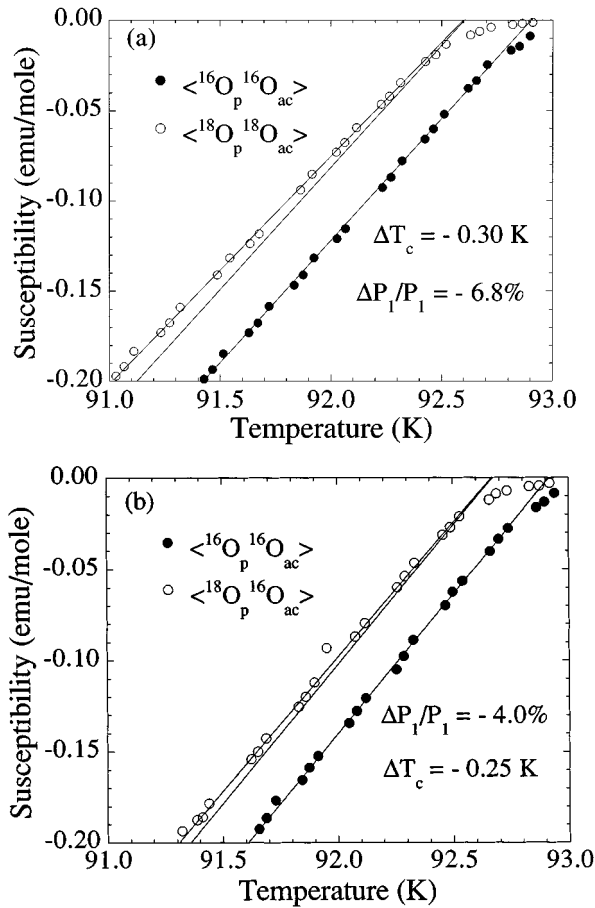


FIG. 2. The susceptibility data near T_c for (a) the standard ^{16}O and ^{18}O samples of $\text{YBa}_2\text{Cu}_3\text{O}_{6.94}$ and (b) the site-selective ^{16}O and ^{18}O samples of $\text{YBa}_2\text{Cu}_3\text{O}_{6.97}$. The slope (denoted by P_1) of the linear portion near T_c for the standard ^{18}O sample is $\sim 6.8 \pm 1.0\%$ smaller than for the standard ^{16}O sample, while the slope for the site-selective ^{18}O sample is $\sim 4.0 \pm 1.0\%$ smaller than for the ^{16}O sample. The in-between straight lines are parallel to the lines for the ^{16}O samples.

for drawing the straight lines can be seen in our previous paper.¹³ We have also shown that the oxygen isotope effect on P_1 (i.e., $\Delta P_1/P_1$) is the same in the measuring fields of 1.0 and 10 Oe, although the magnitude of P_1 does depend on the measuring field slightly.¹³ This suggests that the observed isotope effect on P_1 is not caused by the difference in the flux pinning of the ^{16}O and ^{18}O samples, which will depend on the measuring field. Also note that the site-selective ^{16}O sample has a larger slope than the standard ^{16}O sample by $\sim 10\%$ due to a larger oxygen content and hole concentration in the site-selective sample.

In Figs. 3(a) and 3(b), we show the susceptibility near T_c for (a) the standard ^{16}O and ^{18}O samples of $\text{Y}_{0.7}\text{Pr}_{0.3}\text{Ba}_2\text{Cu}_3\text{O}_y$ and (b) the site-selective ^{16}O and ^{18}O samples of $\text{Y}_{0.7}\text{Pr}_{0.3}\text{Ba}_2\text{Cu}_3\text{O}_y$. The T_c shift of the plane-site ^{18}O -substituted sample is -1.46 K, while the T_c shift of the fully ^{18}O -substituted sample is -1.70 K. The result indicates that the main contribution ($\geq 85\%$) to the oxygen isotope effect comes from the planar oxygen. From Figs. 3(a) and 3(b), we can also see the differences in P_1 of the underdoped ^{16}O and ^{18}O samples.

It is known that the Meissner fraction $f(T)$ for fine-

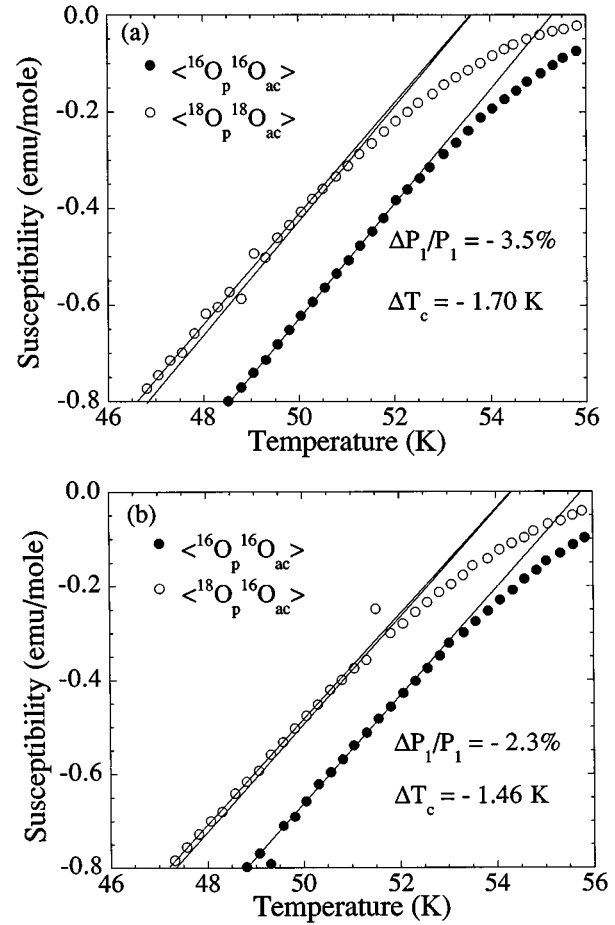


FIG. 3. The susceptibility data near T_c for (a) the standard ^{16}O and ^{18}O samples of $\text{Y}_{0.7}\text{Pr}_{0.3}\text{Ba}_2\text{Cu}_3\text{O}_y$ and (b) the site-selective ^{16}O and ^{18}O of $\text{Y}_{0.7}\text{Pr}_{0.3}\text{Ba}_2\text{Cu}_3\text{O}_y$. The slope of the linear portion for the standard ^{18}O sample $\sim 3.5 \pm 1.0\%$ smaller than for the standard ^{16}O sample, while the slope of the site-selective ^{18}O sample is $\sim 2.3 \pm 1.0\%$ smaller than for the ^{16}O sample.

grained and decoupled samples is reduced due to the penetration depth which is comparable with the radii of grains. We have shown that the slope of the linear portion near T_c is given by¹³

$$P_1 = df(T)/dT \propto R^2/T_c \lambda(0)^2, \quad (1)$$

where R is the average radius of grains and $\lambda(0)$ is the effective penetration depth at zero temperature. Equation (1) is valid when the temperature is higher than T^* (above which complete field-induced grain decoupling has occurred) and T_{eff} , at which $\lambda = R$, $f(T_{\text{eff}}) = R^2/15\lambda^2 = 1/15$,¹⁴ or $\chi(T_{\text{eff}}) \sim 0.8$ emu/mol (without correcting for a demagnetization factor of 1/3). Since there is a small oxygen isotope effect on T_c for the optimally doped samples, the large oxygen isotope effect on P_1 indicates that there is a large oxygen isotope effect on the penetration depth (the average grain radii of the ^{16}O and ^{18}O samples must be the same since they are from the same pellet and have the same susceptibility before isotope exchange). From Eq. (1), we obtain

$$\Delta P_1/P_1 = -\Delta T_c/T_c - 2\Delta\lambda(0)/\lambda(0), \quad (2)$$

where Δ means the isotope-induced change. From Eq. (2), and Fig. 2, we obtain $\Delta\lambda(0)/\lambda(0) \sim +3.5\%$ for the fully isotope-substituted sample and $\sim +2.0\%$ for the plane-site ^{18}O -substituted sample with $x=0$. So the oxygen in the CuO_2 plane sites contributes to $\sim 4/7$ of the total oxygen isotope effect on the penetration depth for the $x=0$ samples. This may indicate that the oxygen from different sites contributes equally to the total oxygen isotope effect on the penetration depth in the optimally doped samples. For the Pr-doped site-selective samples, almost all the shift in T_c can be associated with the shift in λ . From Eq. (2) and Fig. 3, we find $\Delta\lambda(0)/\lambda(0) \sim +3.5\%$ for the fully ^{18}O -substituted sample and $\sim +2.4\%$ for the plane-site ^{18}O -substituted sample.

An oxygen isotope effect on $\lambda(0)$ has been predicted by a scenario⁹ where the hole concentration depends on the mass of the *apical* oxygen. In Ref. 9, Kresin and Wolf assumed a large asymmetry in the double-well potential for the apical oxygen and showed that the hole concentration would depend on the mass of the apical oxygen. If their model were true, there would be negligible oxygen isotope effects on T_c and the penetration depth in the underdoped site-selective samples where ^{18}O atoms are in the plane sites and ^{16}O atoms in the apical and chain sites. This is in contradiction with our experimental result [see Fig. 3(b)]. So it is unlikely that there are effects of the *apical* oxygen mass on the hole concentration and, therefore, on λ and T_c .

The alternative explanation is that the effective mass of carriers depends on the oxygen mass. Evidence of this has been shown in our recent paper.¹³ The ion-mass dependence of the effective mass is connected to the polaronic effect due to the breakdown of the Migdal approximation.¹⁵ The strong interaction of the electrons with optical phonons narrows the electronic bandwidth and enhances the effective mass of carriers by a factor $A(\omega)\exp(B/\omega)$, where $A(\omega)$ has a weak dependence on ω and B is a constant depending on the electron-phonon coupling constant.¹⁵ The enhancement factor depends on the ion mass, and so there is an isotope effect on the effective mass of carriers.

In summary, we have observed a large oxygen isotope shift in the underdoped site-selective samples of $\text{Y}_{0.7}\text{Pr}_{0.3}\text{Ba}_2\text{Cu}_3\text{O}_y$, where ^{18}O atoms are in the plane sites and ^{16}O atoms in the apical and chain sites. We show that the oxygen in the CuO_2 plane sites predominantly contribute to the total oxygen isotope shifts of T_c in the optimally doped $\text{YBa}_2\text{Cu}_3\text{O}_y$ and underdoped $\text{Y}_{0.7}\text{Pr}_{0.3}\text{Ba}_2\text{Cu}_3\text{O}_y$. We also show that there is an oxygen isotope effect on the penetration depth for the fully and site-selectively substituted samples, which can be explained as due to an oxygen isotope effect on the effective mass of carriers. Our results thus confirm that the oxygen or related phonons in the CuO_2 planes are important to the superconductivity and will place a strong constraint on the high- T_c pairing mechanism.

*Present address: Physik-Institut der Universität Zürich, CH-8057 Zürich, Switzerland.

¹B. Batlogg *et al.*, Phys. Rev. Lett. **58**, 2333 (1987).

²L. C. Bourne *et al.*, Phys. Rev. Lett. **58**, 2337 (1987).

³J. H. Nickel, D. E. Morris, and J. W. Ager, Phys. Rev. Lett. **70**, 81 (1993).

⁴M. K. Crawford *et al.*, Phys. Rev. B **41**, 282 (1990).

⁵H. J. Bornemann and D. E. Morris, Phys. Rev. B **44**, 5322 (1991).

⁶J. P. Franck *et al.*, Phys. Rev. B **44**, 5318 (1991).

⁷J. P. Franck, S. Harker, and J. H. Brewer, Phys. Rev. Lett. **71**, 283 (1993).

⁸K. J. Leary *et al.*, Phys. Rev. Lett. **59**, 1236 (1987).

⁹V. Z. Kresin and S. A. Wolf, Phys. Rev. B **49**, 3652 (1994).

¹⁰D. Zech *et al.*, Nature **371**, 681 (1994).

¹¹J. D. Jorgensen *et al.*, Phys. Rev. B **41**, 1863 (1990).

¹²K. Conde *et al.*, Physica C **210**, 282 (1993).

¹³Guo-meng Zhao and Donald E. Morris, Phys. Rev. B **51**, 16 487 (1995).

¹⁴A. M. Neminsky *et al.*, Phys. Rev. Lett. **72**, 3092 (1994).

¹⁵A. S. Alexandrov and N. F. Mott, Int. J. Mod. Phys. B **8**, 2075 (1994).